Proceedings of the ASME 2010 10th Biennial Conference on Engineering Systems Design and Analysis
ESDA2010
July 12-14, 2010, Istanbul, Turkey

ESDA2010-24599

MODELLING AND VALIDATION OF A ROTOR SYSTEM WITH BALL BEARINGS

Onur Cakmak
Istanbul Technical University,
Faculty of Mechanical Engineering
80191, Gumussuyu, Istanbul, TURKEY
E-mail: cakmakon@yahoo.com

Kenan Y. Sanliturk
Istanbul Technical University,
Faculty of Mechanical Engineering
80191, Gumussuyu, Istanbul, TURKEY
E-mail: sanliturk@itu.edu.tr

ABSTRACT

In this paper, a dynamic model of a rotor-ball bearing system is developed in Msc. ADAMS commercial software. Contacts between the balls and the rings are modelled according to Hertzian theory. The bearing model is capable of representing the effects of bearing defects and internal clearances. When they are coupled with the rotor structures, bearings without any defect can also cause excessive vibrations due to the resonance characteristics of the system. In order to demonstrate these characteristics the rotor itself is modelled as a flexible shaft and a disc positioned at the free end of the shaft. The rotor-ball bearing model developed here is capable of representing the gyroscopic effects and the behaviour of the system under different unbalance conditions. Various case studies are performed and Campbell diagrams are obtained by using short-time Fourier transform method.

A test rig consisting of two ball bearings, a shaft and a disc is also designed and developed so as to validate the theoretical model using experimental data. The test rig is developed in such a way that all of the elements are easy to assemble/disassamble, allowing quick observation of the system's dynamic behaviour for different parameters including imbalance, internal clearance and bearing defects. Modal analysis and order tracking analysis were carried out using the test rig. Both the modal results and Campbell diagrams obtained using experimental data are compared with their theoretical counterparts. In the light of the experimental data, the theoretical model is validated for the purpose of further analyses and research.

1. INTRODUCTION

In many mechanical engineering applications, including the production plants, automotive industries and household appliances, ball bearings are the most common components. For the purposes of condition monitoring, fault diagnostics and system maintenance of a rotating machinery, vibration generation and transmission through rolling bearings is a very important subject to study [1]. Also rolling bearings have very significant effects on the dynamics and vibrations of mechanical systems, hence understanding the dynamic behaviour of ball bearings is very important.

In most of the published literature, vibrations generated and caused by ball bearings are studied when the bearings are defected [1-3]. Distributed and localized defects on ball bearing's rings and rolling elements cause excessive vibrations. It is very well-known that for fault diagnostics and system maintenance issues vibration behaviour of a ball bearing can give important clues. Tandon and Choudry [1] in 1997 studied the vibration response of rolling element bearings due to a localized defect in an analytical manner. They assumed that the bearing rings are isolated continuous systems and obtained the equations of motion by using Lagrange's equations. The localized defects are assumed as pulse generators and these pulses are mentioned as generalized forces in the Lagrange's equations. Sassi et al. [2] tried to cope with the damaged bearing vibration phenomena in a numerical manner. Just like Tandon et al. they used the impact assumption for defect dynamics. In addition stiffness and damping of the lubricant fluid film has been taken into consideration. Tandon et al. [3] also studied the vibrations of ball bearings with distributed defects. First, they obtained the vibration response of a bearing without any defect. They determined the amplitude of the vibration at cage frequency and its harmonics by using a Fourier series expansion. They also compared the defected and the ideal models. Their results showed that outer and inner races have a response having a spectrum with peaks at characteristic defect frequencies for respective races.

The effects of radial clearance, number of balls and preload are also studied by many others [4-7]. Tiwari et al. [4] had a study about the effect of radial clearance to vibration response of a balanced rotor. The differential equations were obtained with an assumption of linearized stiffness [5]. The equation was solved by using Cash-Kord Runge-Kutta method. Tiwari et al. [6] improved their model at reference [4] for the case of unbalance. Aktürk et al. [7] studied the effects of balls and preload on bearing vibrations. For a system with no defects a theoretical investigation was made in order to determine whether the amount of preload and the change in number of balls could reduce the effects of ball-passing vibrations. The stiffness was determined with the Hertzian contact approach. In conclusion they showed that the number of balls and preload were critical parameters that affected ball bearing vibrations and should be considered when modelling bearings.

Computer aided simulations are also used in bearing models built until now. Some of the studies [2] are about toolboxes created on the environments of MATLAB or Mathematica. On the other hand, Wensing [8] built a ball bearing model by using Component Mode Synthesis (CMS) method. That study also contains the experimental validation of the model. Sopanen et al. [9, 10] built a model with the help of Multi-Body System approach using MSC. ADAMS. They affirm that, with this approach it is possible to model the rotor as flexible to observe the effects of individual components on the total response. Also the misalignments and waviness of the rings can be implemented into the model. Several experimental methods are being used for measuring the vibrations caused by bearings. In the literature, the main objective of these experimental methods is to detect the defects of bearings [12, 13]. However, there are also experimental studies made in order to validate numerical models [8], [11].

This paper introduces a new model of a rotor-ball bearing system. In this paper, it is aimed to create a new model for a rotor-bearing system, which can demonstrate not only the vibrations generated by a ball bearing itself, but also the effect of the flexible shaft and rigid disc structure on the resonance characteristics of the system. A numerical modal analysis is performed and Frequency Response Functions (FRF) are obtained. Also, the change of natural frequencies with respect to rotational speed due to gyroscopic effects is observed. The Campbell diagrams are obtained using the data generated from the model by using Short-Time Fast Fourier Transform (STFT) technique for the case in which the gyroscopic effects are included. For experimental validation process, a test rig is designed with an overhung rotor supported by two ball bearings. Experimental modal analysis and order tracking analysis techniques are followed during this process. The case studies with differing unbalance masses are also carried out for further analyses.

The outline of this paper is as follows. First, a review of the determination of contact stiffness and damping between ball bearing elements is given. Then, the kinematics of a ball bearing and defect frequencies are briefly described. The assumptions and methodology used on the modelling process of the rotor-ball bearing system are introduced. After that, in the next step, the test rig and the experimental procedures are described. Finally, the results of the numerical model and experimental data are compared. For the static case experimental and numerical Frequency Response Functions (FRF) are presented. For the dynamic case, experimental and theoretical Campbell diagrams are obtained. The measured and predicted results are compared and discussed.

2. THEORETICAL BACKGROUND

2.1 Contact Stiffness and Damping at Ball Bearings

Loads acting between the rolling elements and raceways develop only small areas of contact [15]. For ball bearings this area is smaller and this kind of contact is named as point contact. Stiffness at these contacts is calculated by using Hertzian Theory. Lubrication must be taken into account when modeling ball bearings that run at high operational speeds. This type of contact is called elastohydrodynamic (EHL) contact. In this study the stiffness and damping effects of the lubrication film are neglected. The assumption made here is based on a dry contact mechanism.

The rolling elements are in contact with the inner and outer raceway in a ball bearing. The surface of a rolling element is convex whereas the surface of the outer raceway is concave. The surface of the inner raceway is convex in the direction of motion and concave in the transverse direction [8]. Figure 1 shows major geometric features of a ball bearing.

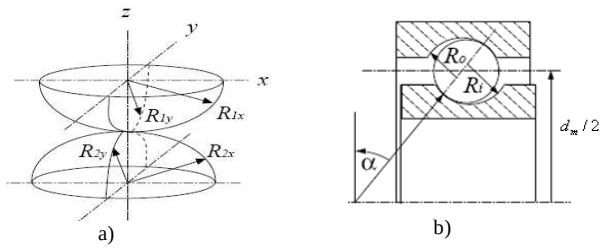

Figure1. a) CONTACTING BODIES b) GEOMETRIC FEATURES OF THE CONTACT REGION OF A BALL BEARING [8]

If R_{re} denotes the radius of the ball itself, the radii of the curvature for the inner contact are:

$$R_{1x} = R_{re} \tag{1}$$

$$R_{1y} = R_{re} \tag{2}$$

$$R_{2x} = \frac{d_m / 2}{\cos(\alpha)} - R_{re} \tag{3}$$

$$R_{2y} = -R_i \tag{4}$$

Similarly, the radii of curvature for the outer contacts are:

$$R_{2x} = -(\frac{d_m/2}{\cos(\alpha)} + R_{re}) \tag{5}$$

$$R_{2y} = -R_o \tag{6}$$

Contact angle α is a parameter which affects the radii of curvature of the raceway. However, as pointed out in [8], the assumption of a zero degree contact angle causes only a small error [8]. Usually, the contact surface in Fig.1 is assumed to be paraboloid. The geometric features between two contacting solids can be expressed in terms of the curvature sum R, and curvature difference R_d, which are described in [8] as

$$\frac{1}{R} = \frac{1}{R_x} + \frac{1}{R_y} \tag{7}$$

$$R_d = R(\frac{1}{R_x} - \frac{1}{R_y}) \tag{8}$$

where

$$\frac{1}{R_x} = \frac{1}{R_{1x}} + \frac{1}{R_{2x}} \tag{9}$$

$$\frac{1}{R_y} = \frac{1}{R_{1y}} + \frac{1}{R_{2y}} \tag{10}$$

When a normal load is applied to the two contacting bodies, the point contact expands to an ellipse [9], as a_e and b_e are semi-minor and semi-major axes of this ellipse geometry, the ellipticity parameter k_e is defined as [17]:

$$k_e = \frac{a_e}{b_e} \tag{11}$$

Also this parameter can be defined as a function of curvature difference R_d and the elliptic integrals of the first ξ and second ζ kind as [16]

$$k_e = \left[\frac{2\xi - \zeta(1+R_d)}{\zeta(1-R_d)}\right]^{1/2} \tag{12}$$

where

$$\xi = \int_0^{\pi/2} \left[1-(1-\frac{1}{k_e^2})\sin^2\varphi\right]^{-1/2} d\varphi \tag{13}$$

$$\zeta = \int_0^{\pi/2} \left[1-(1-\frac{1}{k_e^2})\sin^2\varphi\right]^{-1/2} d\varphi \tag{14}$$

where φ is an auxiliary angle. As can be seen, an iteration procedure is required in order to determine the ellipticity parameter and elliptic integrals. One point numerical iteration and curve fitting techniques can be used and approximation formulae given below can be obtained [9]:

$$\bar{k}_e = 1.0339\left(\frac{R_y}{R_x}\right)^{0.6360} \tag{15}$$

$$\bar{\xi} = 1.0003 + 0.5968\frac{R_x}{R_y} \tag{16}$$

$$\bar{\zeta} = 1.5277 + 0.6023\ln\left(\frac{R_y}{R_x}\right) \tag{17}$$

The contact stiffness coefficient for the elliptical contact assumption can be calculated as [9]:

$$K_c = \pi\bar{k}_e A E' \sqrt{\frac{R\bar{\xi}}{4.5\bar{\zeta}^3}} \tag{18}$$

where the effective modulus of elasticity, E', is defined as:

$$\frac{1}{E'} = \frac{1}{2}\left(\frac{1-\upsilon_1^2}{E_1} + \frac{1-\upsilon_2^2}{E_2}\right) \tag{19}$$

E is the modulus of elasticity and υ is the Poisson's ratio and the subscripts refer to solids 1 and 2. In the case of ball bearing, both of the solids have the same elasticity properties [9].

In ball bearings the main cause for the damping is the lubricant film in contacts. Also material damping at contact region is another factor. In the proposed model a constant damping value, based on the experimental data, is used due to the relatively small damping in the bearing.

2.2 Kinematics of a Ball Bearing

Unlike hydrodynamic or hydrostatic bearings, motions occurring in ball bearings are not restricted to simple movements [15]. Different components have different rotational speeds and velocities. This situation causes excitations at different frequencies called "defect frequencies" and they can be very significant when the component is defected. It is also known that bearing without any defect generates vibrations at Ball Passing Frequency (BPF) which has the same value with

outer ring defect frequency. If n_i and n_o denote the rotational speeds of inner and outer rings (in rpm) , d indicates ball diameter and α indicates contact angle, N_b is the number of balls, then the so-called defect frequencies are given as follows.

Fundamental Train Frequency (Cage speed):

$$FTF = \frac{1}{2}[n_i(1-\frac{d\cos\alpha}{d_m}) + n_0(1+\frac{d\cos\alpha}{d_m})] \tag{20}$$

Ball pass frequency outer ring:

$$BPFO = \frac{N_b}{120}[(n_i - n_0)(1-\frac{d\cos\alpha}{d_m})] \tag{21}$$

Ball pass frequency inner ring:

$$BPFI = \frac{N_b}{120}[(n_i - n_0)(1+\frac{d\cos\alpha}{d_m})] \tag{22}$$

Ball spin frequency:

$$BSF = \frac{N_b}{120}[\frac{d_m}{d}(n_i - n_0)(1-(\frac{d\cos\alpha}{d_m})^2] \tag{23}$$

3. DYNAMIC MODELLING

3.1 Model for the ball bearing

During the modelling process a particular type of deep-groove ball bearing is used. The rings and rolling elements are assumed to be rigid. As mentioned before, dry contact mechanism is assumed here. It is also assumed that the rolling elements are rolling on the raceways without slipping. The stiffness of the contacts is determined via the Hertzian contact theory as explained in section 2. The cage structure is included in the ball bearing model as rigid connectors. The complete model of the ball bearing is shown in Fig. 2.

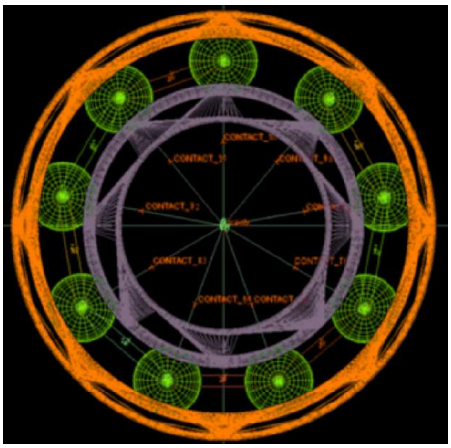

Figure 2. MODEL OF THE BALL BEARING, CREATED ON MSC. ADAMS COMMERCIAL SOFTWARE

3.2 Model for the rotor-bearing assembly

After the ball bearing model is built, a Finite Element (FE) model for a shaft, shown in Fig. 3, is created. The shaft is assumed to be flexible and it is represented using elastic beam elements with circular cross sections. The rotor also contains a disc with 300 mm diameter and 20 mm thickness. The inertial properties of the disc are calculated and implemented in the model and the disc is assumed to be rigid with specified mass and moments of inertia properties. At first, a primitive FE model for the rotor-bearing shown in Fig. 4 is developed and in this model spherical and cylindrical joints are used instead of ball bearings. Spherical joint has three degrees of freedom which are all rotational whereas cylindrical joint has only one freedom which is the rotation about the axial direction.

After developing the primitive model, flexible shaft with beam elements and the ball bearing model described in section 3.1 are assembled. In practice, deep groove ball bearings have three rotational degrees of freedom. The inner ring can have very limited rotational capacity around both radial axes. In the model this freedom can be satisfied with the joint between the shaft and the inner ring. A bushing element with rotational stiffness is used for joining the shaft with the bearing. Numerical FRFs are then calculated using the model developed.

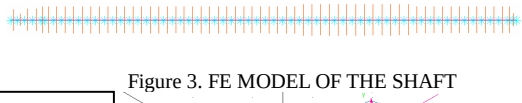

Figure 3. FE MODEL OF THE SHAFT

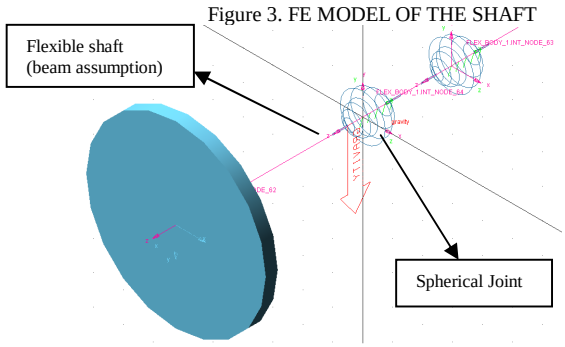

Figure 4. PRIMITIVE MODEL WITH SPHERICAL JOINTS INSTEAD OF BEARINGS

Once the numerical modal analysis is performed for the static case, the model is run-up to 1200 rpm in 10 seconds and time-domain acceleration data are collected. This dynamic analysis is also carried out for a given level of unbalance on the disc. A Short Time Fast Fourier Transform (STFT) is applied to this time data and the results are obtained as Campbell diagrams.

4. TEST RIG AND MESAUREMENTS

In order to validate the rotor-ball bearing model developed in this paper, a test rig shown in Fig. 5 is designed. The test rig comprises a rotor part (a shaft and a disc at the end) and two deep groove ball bearings supporting the rotor. As can be seen in Fig. 5, the ball bearings are mounted on a heavy block with soft supports. The system is driven by an AC motor and the power transmission is provided by a belt-pulley mechanism. AC motor is separated from the whole system and fixed to the ground. The test rig is designed in such a way that it is easy to change some components in the assembly. Shafts with different lengths can be used and the ball bearings can be replaced with others with different clearance values. Unbalance masses can easily be added to the structure via the holes on the disc. Motor can be positioned precisely so as to calibrate the belt tension. The assembly of the shaft and the disc is done by using a special key design and an additional nut at the free end of the shaft.

Using the test rig developed FRF measurements for the static case is carried out first. The structure is excited using a modal impact hammer and charge type accelerometers are used to measure the response. An analyser with proper signal conditioning hardware is used. After the static measurements the system is run-up to 1200 rpm. Order tracking analyses are performed, both order and Campbell diagrams are obtained. Information about the rotational speed is obtained by using the signal from an existing taco probe on the AC motor and the belt ratio. The accuracy of this taco signal is verified using another laser tachometer tracing the rotation of the disc directly. Accelerometers are positioned on the block housings and vibrations on various directions are collected. Forced response of the system is measured when the system is excited by known levels of unbalance. Repeatability checks are performed and calibration of the system is checked before each experiment during both static and dynamic measurements.

Figure 5. THE TEST RIG

5. RESULTS AND DISCUSSION

FRFs are measured using the test rig and corresponding FRFs are calculated using the model developed for comparison purposes. Sample results are presented in Figures 6 and 7. Figure 6 shows the numerical and measured FRFs obtained in vertical -y- direction whereas Fig. 7 demonstrates those in horizontal -x- direction. It should be noted that there are 3 predicted FRFs in each figure, individual predictions corresponding to 3 different bearing models. As mentioned before, two of these predictions are based on so-called primitive models using cylindrical and spherical joints in order to model the bearings. The third prediction is based on the ball bearing model given in Fig. 2. Theoretically, when the system is assumed to be homogeneous, the natural frequencies for the bending modes in horizontal and vertical directions should be the same, as in the first primitive model with spherical joints. However, this is not observed for the real system because of the different stiffness characteristics of the block housings and the belt connection along horizontal and vertical directions. The experimentally observed behaviour of the system is represented in the model by using springs and bushing elements in various directions..

Another important result is the difference between the predictions obtained from the primitive rotor model and the new ball bearing model. In many published work, there is a general assumption that spherical or cylindrical joints can be used to model roller bearings especially when they are fixed to the ground. However, as can be seen in Figures 6 and 7 there is a very significant difference between the natural frequencies obtained from those primitive models and experiments. For the model with cylindrical joint it can be said that this model is over constrained, hence the natural frequencies, especially those for the second bending modes are quite higher than the real values. On the other hand, spherical joints have additional (rotational) freedoms and this results in decrease in over predictions of natural frequencies. The translational and rotational stiffnesses of ball bearing, housing and belt are taken into account in the improved model.

The damping of the system at different frequencies are modelled in the light of the experimental data. In other words, the measured damping levels are used in the numerical model. As seen in Figures 6 and 7, this leads to satisfactory predictions of the peak amplitudes when compared to the experimental results. However, the results obtained using the primitive models are poor since the stiffness and damping of the housings are not included in those models.

The experimental FRFs in Figures 6 and 7 show several peaks indicating natural frequencies.. The one at 16 Hz is the natural frequency corresponding to the mode shape that can be described as the rocking of the whole system as a rigid body on elastic supports of the heavy bench and it is not included in the theoretical models. Another peak at 46 Hz in the measured FRFs corresponds to the torsional mode of the structure. The

torsional mode appears here due to the impact hammer excitation having tangential component during the measurement. This causes torsional response of the system and appears as a peak in the measured FRF. In order also to observe this torsional mode in the theoretical models, the system is excited in a way that enables significant angular vibration. The other peaks in the measured FRFs represent the first and the second bending modes of the system. It is noted that the measured and the predicted natural frequencies for the torsional and bending modes agree quite well for the case when the ball bearing model depicted in Fig. 3 used. The torsional mode is not affected by the bearing hence the the primitive models are are capable of predicting the natural frequency of the torsional mode accurately. However, predicted natural frequencies for the bending modes are far from reality when the primitive bearing models are used.

After the static FRF analyses, the system is investigated under rotating condition.. The rotational speed of the system is gradually increased and the response of the system is recorded during this process. The same situation is simulated using the numerical model. In both cases, the data captured are processed to obtain the Campbell diagrams. The experimental numerical results are presented in Figures 8 and 9, respectively.

It is seen in Figures 8 and 9 that because of the imbalance, the 1st harmonic is very dominant. It should also be noted that for the ball bearing studied here, the ratio between the Ball Passing Frequency and shaft rotation speed can be calculated from Eqn. (21) as 3.55 In both experimental and numerical cases, the BPFO can be seen. However, they are not very significant as the bearings used can be considered defect free.

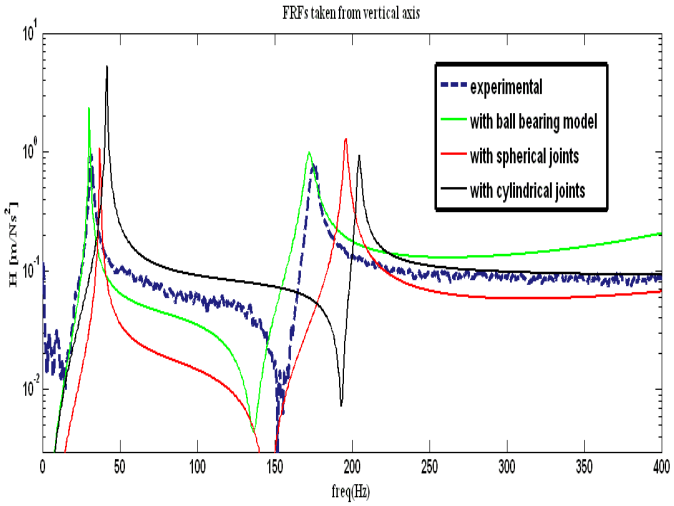

Figure 6. COMPARISON OF THE RESPONSES OF THE MODELS AND TEST RIG FOR AN IMPACT IN VERTICAL DIRECTION

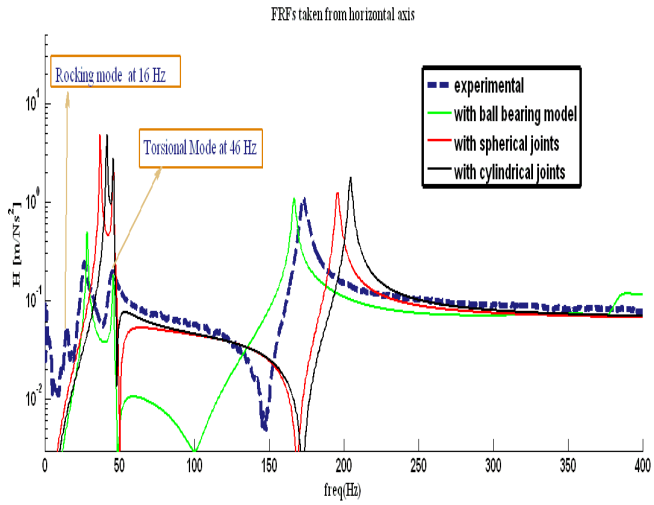

Figure 7. COMPARISON OF THE RESPONSES OF THE MODELS AND TEST RIG FOR AN IMPACT IN HORIZONTAL DIRECTION

Also, the natural frequencies can be identified in both figures. It appears in the numerical result that the first bending modes is dominant at lower rotational speeds. A possible reason for this might be the use of undamped model during the forced response calculations. In experimental Campbell diagram the 1st bending modes are less dominant, but they can be observed when some harmonics of the running speed or ball pass frequency coincide with them. Also, as expected, when the higher harmonics (7th, 8th, 9th …) coincide with the second bending natural frequencies, higher levels of vibrations are obtained. In the numerical case, vibrations levels at these higher frequencies are overestimated possibly due to smearing effect. A "numerical order tracking" can be a solution for this situation.

During the run-up procedure, the natural frequencies of the system corresponding to bending modes split from each other. This situation is a result of the gyroscopic effects which are more significant for overhung rotors [19].

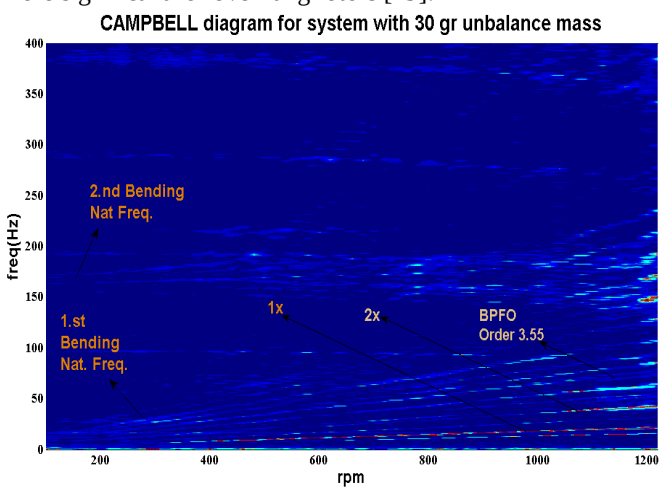

Figure 8. CAMPBELL DIAGRAM OBTAINED FROM THE EXPERIMENTS

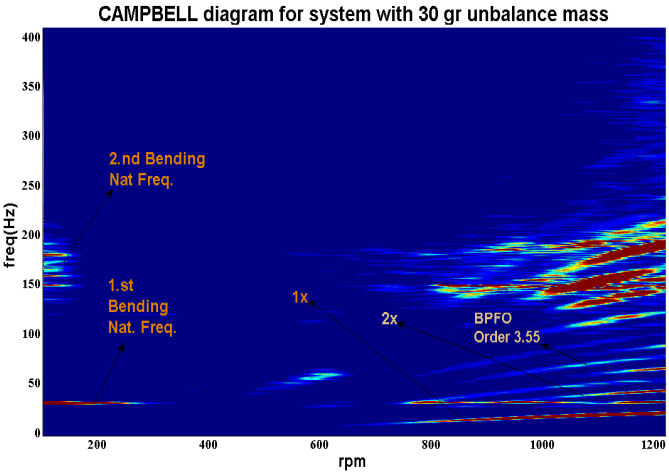

Figure 9. CAMPBELL DIAGRAM OBTAINED FROM THE NUMERICAL MODEL

In order to demonstrate these gyroscopic effects and to determine the natural frequencies, a linearization [20] process is carried out and an eigensolution are obtained at certain running speeds. The bending natural frequencies at each rpm values for both experimental and numerical run-up procedures can be seen in Figures 8 and 9. The natural frequency split due to gyroscopic effects is visible especially for the 2nd bending modes. However, the natural frequency split for the 1st bending modes is not very significant.

6. CONCLUDING REMARKS

A new dynamic model is developed in order to demonstrate the vibration behaviour of a rotor-ball bearing system. A test rig is designed and developed to carry out the validation process. It is shown that for the rotor-ball bearing systems the stiffness of the bearings and housings are important parameters in predicting the modal properties and dynamic behaviour.

The model is also run-up to 1200 rpm. The Campbell diagrams obtained by using STFT techniques showed satisfactory results. There are peaks at outer ring ball passing frequencies and harmonics of the running speeds. The critical speeds are shown in both numerical and experimental results.

It can be said that the new bearing model has some features necessary for modelling the response characteristics of a rotor-bearing system. It is obvious, however, that the current numerical model has some limitations. Current work is directed towards improving the rotor-bearing model and the associated analyses.

REFERENCES

[1] Tandon N., Choudhury A., 1997. “An Analytical Model For the Prediction of the Vibration Response of Rolling Elements Due to Localized Defect”, Journal of Sound and Vibration, Volume 205(3), pp. 275-292.

[2] Sassi S., Badri B., and Thomas M., 2007. “A Numerical Model to Predict Damaged Bearing Vibrations”, Journal of Vibration and Control, Volume 13, pp. 1603-1630.

[3] N Tandon N., Choudhury A., 1998. “A Theoretical Model To Predict Vibration Response of Rolling Elements Due to Distributed Defects Under Radial Load”, Journal of Vibration and Acoustics, Volume 120, pp. 214-220.

[4] Tiwari M., Gupta K., 2000. “Effect of Radial Internal Clearance of a Ball Bearing On The Dynamics Of A Balanced Horizontal Rotor”, Journal of Sound and Vibration, Volume 238(5), pp. 723-756.

[5] Tamura H., Tsuda Y., 1985. “On The Static Running Accuracy of Ball Bearings”, Bulletin of the JSME, Volume 28, pp. 1240-1246.

[6] Tiwari M., Gupta K., 2000. “Dynamic Response of An Unbalanced Rotor Supported on Ball Bearings”, Journal of Sound and Vibration, Volume 238(5), pp. 757-779.

[7] Aktürk N., Uneeb M., and Gohar R., 1997. “The Effects of Number of Balls and Preload on Vibrations Associated With Ball Bearings”, Journal of Tribology, Volume 1119, pp. 747-753.

[8] Wensing J.A., 1998, “On the Dynamics Of Ball Bearings”, Phd Thesis, University of Twente, the Netherlands.

[9] Sopanen J., Mikkola A., 2003 “Dynamic Model of a Deep Groove Ball Bearing Including Localized and Distributed Defects, Part 1: Theory”, Proceedings of the Institution of Mechanical Engineers, Journal of Multi-body Dynamics, Volume 217, 4, pp. 201-211.

[10] Sopanen J., Mikkola A., 2003 “Dynamic Model of a Deep Groove Ball Bearing Including Localized and Distributed Defects, Part 2: Implementation and Results”, Proceedings of the Institution of Mechanical Engineers, Journal of Multi-body Dynamics, Volume 217, 4, pp. 211-221.

[11] Royston T. J., Basdogan I., 1998 “Vibration Transmission Through Self-Aligning (Spherical) Rolling Element Bearings: Theory and Experiment” Journal of Sound and Vibration, Volume 215 5, pp. 997-1014.

[12] Tandon N., Choudhury A., 1999, “A Review of Vibration and Acoustic Measurement Methods for the Detection of Defects in Rolling Element Bearings”, Tribology International, Volume 32, pp. 469-480.

[13] Courrech J., 2000, “Envelope Analysis For Effective Rolling Element Fault Detection- Fact or Fiction?” Brüel & Kjaer Technical Review, Uptime Magazine, Volume 8.

[14] Gade S., Herlufsen H., Hansen H.K., 1995, “Order Tracking Analysis” Brüel & Kjaer Technical Review, No 2.

[15] Harris T. A., 1993, *“Rolling Bearing Analysis”*, Wiley & Sons, New York, USA, Chap. 2.

[16] B. J. Hamrock 1994, *“Fundamentals of Fluid Film Interaction”*, Mc-Graw Hill,, New York.

[17] Hamrock B. J., Dawson D., 1976 “Isothermal Elastohydrodynamic Lubrication of Point Contacts, Part 1:

Theoretical Formulation", Journal of Lubrication Technology., Volume 98, pp. 223-229.
[18] Kramer E., 1993 "*Dynamics of Rotors and Foundations*. Springer-Verlag., New York, USA.
[19] Goodwin J. M., 1989 "*Dynamics of Rotor-Bearing Systems*", Unwin Hyman Ltd., London, U.K., Chap. 4.
[20] Ortiz J. L., Bir G. S., 2006 "Verification of New MSC.ADAMS Linearization Capability For Wind Turbine Applications" 44th AIAA Aerospace Sciences Meeting and Exhibit, Reno, Nevada, US